



DEC 22 1946

copy!  
ACR No. L4H07

NATIONAL ADVISORY COMMITTEE FOR AERONAUTICS

# WARTIME REPORT

ORIGINALLY ISSUED  
August 1944 as  
Advance Confidential Report L4H07

CHARTS FOR ESTIMATION OF THE CHARACTERISTICS  
OF A HELICOPTER ROTOR IN FORWARD FLIGHT

I - PROFILE DRAG-LIFT RATIO

FOR UNTWISTED RECTANGULAR BLADES

By F. J. Bailey, Jr. and F. B. Gustafson

Langley Memorial Aeronautical Laboratory  
Langley Field, Va.



**NACA**

WASHINGTON

**N A C A LIBRARY**

LANGLEY MEMORIAL AERONAUTICAL  
LABORATORY  
Langley Field, Va.

NACA WARTIME REPORTS are reprints of papers originally issued to provide rapid distribution of advance research results to an authorized group requiring them for the war effort. They were previously held under a security status but are now unclassified. Some of these reports were not technically edited. All have been reproduced without change in order to expedite general distribution.

NATIONAL ADVISORY COMMITTEE FOR AERONAUTICS

ADVANCE CONFIDENTIAL REPORT

CHARTS FOR ESTIMATION OF THE CHARACTERISTICS

OF A HELICOPTER ROTOR IN FORWARD FLIGHT

I - PROFILE DRAG-LIFT RATIO

FOR UNTWISTED RECTANGULAR BLADES

By F. J. Bailey, Jr. and F. B. Gustafson

SUMMARY

Charts showing the rotor profile drag-lift ratio are presented for a helicopter rotor operating in forward flight and having hinged rectangular untwisted blades. Charts are given for a range of power input covering glides, level flight, and moderate rates of climb. Each chart expresses the relation between the lift and the profile-drag characteristics of the rotor for various combinations of pitch angle, tip-speed ratio, and solidity for a particular value of a parameter representing the shaft power input.

A particular drag curve, represented by a power series, was used in preparing the charts. This curve is compared with experimental curves for typical airfoils. The method by which the charts may be used in calculating the total shaft power required for any specific flight condition is shown by an example.

The charts indicate that, for the rotor with rectangular untwisted blades, one effect of increasing the shaft power input is to produce a moderate increase in the profile drag-lift ratio. They further indicate, that, regardless of the amount of power used, the optimum profile drag-lift ratio is obtained at the highest pitch angles permitted by the high section angles of attack encountered on the retreating side of the rotor disk.

## INTRODUCTION

Because of the pressing requirements of procurement agencies for a rational method for evaluation of helicopter proposals and because of the requirements of helicopter designers for a basis for choosing the optimum combination of variables, it was felt that a need existed for design charts summarizing the effect of changes in the major variables on the characteristics of a powered rotor in forward flight. The method of analysis of reference 1 accordingly was used to prepare summary charts that are generally similar to figure 3 of reference 1 but cover various amounts of shaft power input. The present report has, for simplicity, been restricted to the basic case of zero blade twist.

## METHOD OF ANALYSIS

Parameter for shaft power input.— The primary modification made herein in the method of reference 1 is the introduction of a new parameter  $P/L$  for rotor-shaft power input. The symbol  $P$  represents the drag that would absorb the same power, at the velocity along the flight path, as the power being supplied through the rotor shaft. The parameter  $P/L$  is therefore equal to the total drag-lift ratio, or

$$\frac{P}{L} = \left(\frac{D}{L}\right)_o + \left(\frac{D}{L}\right)_i + \left(\frac{D}{L}\right)_p + \left(\frac{D}{L}\right)_c \quad (1)$$

where

$\left(\frac{D}{L}\right)_o$       profile drag-lift ratio

$\left(\frac{D}{L}\right)_i$       induced drag-lift ratio

$\left(\frac{D}{L}\right)_p$       parasite drag-lift ratio

$\left(\frac{D}{L}\right)_c$       drag-lift ratio representing angle of climb;  
that is, rate of climb divided by velocity  
along flight path

Charts showing values of  $(D/L)_0$  can be calculated by the method outlined in reference 1 for any desired value of  $P/L$  by inclusion of the shaft-torque coefficient

$$\frac{2C_Q}{\sigma} = \frac{P}{L} a \left( \mu \frac{2C_T}{\sigma a} \right)$$

where

- $C_Q$  torque coefficient
- $\sigma$  solidity; ratio of total blade area to swept-disk area
- $a$  slope of lift coefficient against section angle of attack (radian measure)
- $\mu$  tip-speed ratio
- $C_T$  thrust coefficient

in the equation expressing the torque equilibrium of the rotor. (See section entitled "Application of Theory" in reference 1.) The expression for  $\mu \frac{2C_T}{\sigma a}$  is given in equation (14) of reference 1.

Rotor characteristics.— The sample rotor for which the charts presented herein were prepared was assumed to have hinged rectangular untwisted blades. A value of the mass factor  $\gamma$  of 15 was used. The charts are considered applicable to rotors having values of  $\gamma$  ranging from 0 to 25.

Airfoil characteristics.— The airfoil characteristics assumed in reference 1 were used in preparing the charts. The equation representing the section profile-drag coefficient is

$$cd_0 = 0.0087 - 0.0216\alpha_0 + 0.400\alpha_0^2$$

where  $\alpha_0$  is the section angle of attack. The corresponding profile-drag curve is shown in figure 1 with experimental curves for several typical airfoils.

Limits of validity of theory.- As was explained in reference 1, calculations based on the representation of the airfoil drag characteristics by a power series of three terms become optimistic when high blade angles are encountered over too large a portion of the rotor disk. It should be noted, however, that very little improvement in  $(D/L)_0$  is to be expected by operating beyond the conditions to which the theory is limited, as a result of the rapidity of growth of the region of high angle of attack. This fact is readily demonstrated by graphical treatments for both autogiro and helicopter cases.

In the example given for the autogiro in reference 1, a satisfactory limit was found to be the condition in which a blade element at an azimuth angle of  $270^\circ$  and having a relative velocity  $u_{TR}$  equal to four-tenths the rotational tip speed reached an angle of attack of  $11.75^\circ$ . The use of this locus line has been retained in the present example but, for convenience, the angle of attack has been increased to an even  $12^\circ$ . Because the limiting angle of attack depends upon the section and upon the Reynolds number and Mach number, an additional locus line has been included for an angle of attack of  $16^\circ$ . For values of  $P/L$  greater than about 0.1, the highest blade angles are encountered at the blade tip instead of inboard; hence, locus lines for angles of attack of  $12^\circ$  and  $16^\circ$  at the blade tip, at an azimuth angle of  $270^\circ$ , are substituted for those for  $u_T = 0.4$  whenever the tip locus lines fall above those for  $u_T = 0.4$ .

In the charts presented herein, the locus lines for the conditions for which a blade element at an azimuth angle of  $270^\circ$  with a relative velocity  $u_{TR}$  equal to four-tenths the rotational tip speed reached a specified angle of attack are designated by the symbol  $\alpha(u_T=.4)(270^\circ)$ . Similarly, the locus lines for the conditions for which the blade tip at an azimuth angle of  $270^\circ$  reached a specified angle of attack are designated by the symbol  $\alpha(1.0)(270^\circ)$ .

## RESULTS

The charts of  $(D/L)_0$  obtained for the sample rotor are shown in figure 2. The chart for  $P/L = 0$ ,

that is, for autorotation, is the same as figure 3 of reference 1 except for the choice of limit lines. A value of  $P/L$  of 0.2 may be considered as typical of present helicopters at or near cruising speed. Values lower than 0.2 correspond to cleaner craft or to a power-on glide. Higher values correspond to less streamlined craft or to a positive angle of climb; the highest value covered by the present charts,  $P/L = 0.5$ , may be viewed as representing a typical helicopter climbing at an angle of approximately  $15^\circ$  or  $20^\circ$ .

### DISCUSSION

Inspection of the charts reveals that the effect of increasing power on the optimum  $(D/L)_o$ , as indicated by the lowest points on the limit lines, is to produce a moderate but progressive increase in the magnitude of the value of  $(D/L)_o$  and to shift the optimum tip-speed ratio toward lower values. It may be remarked that similar charts for twisted blades show a relatively insignificant increase in  $(D/L)_o$ , up to values of  $P/L$  of 0.2 or higher.

As has already been noted, for both helicopter and autogiro conditions, the optimum  $(D/L)_o$  is indicated as being obtained at the highest pitch angles permitted by the section angles of attack encountered on the retreating side of the rotor disk. The choice of pitch angles materially lower than those corresponding to the locus lines for an angle of attack of  $12^\circ$  results in extreme inefficiency.

### SAMPLE PERFORMANCE CALCULATION

Power absorbed by main rotor.— In order to illustrate the manner in which the charts may be used to estimate the power required by a helicopter under a given set of conditions, an example has been included.

Assume a helicopter to be operating in level flight at sea level under the following conditions:

Forward speed, feet per second.....	80
Tip-speed ratio, $\mu$ .....	0.2
Disk loading, pounds per square foot .....	2.5

400 fms  
Disc Area 1256 sq ft

$$\text{BLADE AREA} = 20 \times 2 \times 2.2 = 88 \text{ sq ft}$$

$$= \frac{3140}{0.001189 \times 1256 \times 80}$$

6 chord 2.2'

NACA ACR No. L4H07

Gross weight, pounds ..... 3140  
 Rotor radius, feet ..... 20  
 Blade plan form ..... Rectangular  
 Blade twist ..... None  
 Solidity ..... 0.07  
 Parasite-drag area, square feet ..... 15

For these assumptions,  $C_L = 0.329$  and  $\frac{C_L}{\sigma} = 4.70$ .

In order to obtain a first approximation to  $(D/L)_0$  for use in equation (1),  $P/L$  is assumed to be 0.2. Figure 2(e) then gives a value of 0.086 for  $(D/L)_0$  at the intersection of the curve for  $\mu = 0.2$  with the line for  $\frac{C_L}{\sigma} = 4.70$ . The value of  $(D/L)_i$ , as indicated in reference 1, is simply  $C_L/4$  or 0.082. The parasite drag-lift ratio is

$$\left(\frac{D}{L}\right)_p = \frac{0.001189 \times 15 \times (80)^2}{3140} = 0.036$$

Since the rate of climb is assumed zero, the value of  $P/L$  from equation (1) is

$$\frac{P}{L} = 0.086 + 0.082 + 0.036 + 0 = 0.204$$

As a second approximation, the value of  $(D/L)_0$  may be obtained by interpolation between the charts for  $\frac{P}{L} = 0.20$  and for  $\frac{P}{L} = 0.25$ . The value so obtained is, within the limits of accuracy in reading the charts, equal to the original value of 0.086 and no further approximations are necessary.

The total rotor-shaft power required for the specified condition may now be calculated as

$$\frac{0.204 \times 3140 \times 80}{550} = 93.2 \text{ horsepower}$$

Power absorbed by auxiliary rotor.- The charts may also be used to estimate the power absorbed by the tail rotor.

Assume that the torque of the main rotor is being counteracted by an articulated auxiliary rotor having the following characteristics:

Blade plan form ..... Rectangular  
 Blade twist ..... None  
 Solidity ..... 0.10

Spindle angle, $\alpha$ , degrees .....	0
Distance between spindle and main rotor axis, feet .....	25
Radius, feet .....	4
Tip-speed ratio .....	0.2

The tail-rotor thrust, based on the main-rotor power already calculated, is 102.7 pounds and the corresponding thrust coefficient  $C_T$  is 0.00536. The inflow-velocity factor  $\lambda$  may be obtained from equation (8) of reference 1

$$\alpha = \frac{\lambda}{\mu} + \frac{C_T}{2\mu^2}$$

Substitution of the values for the present case gives a value of  $\lambda = -0.0134$ . By using a lift-curve slope  $a$  of 5.73 per radian, substitution of this value of  $\lambda$  in equation (6) of reference 1 gives a blade pitch angle  $\theta$  of  $4.47^\circ$ .

In order to permit the use of the charts of figure 2, it is convenient to calculate the value of  $C_L/\sigma$  from the relation

$$\frac{C_L}{\sigma} = \frac{2C_T}{\sigma\mu^2}$$

which gives a value of  $\frac{C_L}{\sigma} = 2.68$ . The value of  $P/L$  corresponding to the specified combination of values  $\mu$ ,  $\theta$ , and  $C_L/\sigma$  is found by interpolation between figures 2(c) and 2(d) to be 0.138.

The auxiliary-rotor shaft power is then

$$\frac{0.138 \times 102.7 \times 80}{550} = 2.1 \text{ horsepower}$$

Since the auxiliary rotor may also be producing a drag, the total power charged to torque counteraction should be calculated from the sum of the values of  $(D/L)_0$  and  $(D/L)_1$ . The value of  $(D/L)_0$  at  $P/L = 0.138$ , by interpolation from figure 2, is 0.120. The value of  $(D/L)_1$  is



$$\begin{aligned}
 \left(\frac{D}{L}\right)_1 &= \frac{C_L}{\sigma} \frac{\sigma}{4} \\
 &= 0.268 \frac{0.1}{4} \\
 &= 0.067
 \end{aligned}$$

The total drag-lift ratio is then 0.187 and the corresponding power is 2.8 horsepower. The difference between the two values of power results from the drag on the auxiliary rotor and hence must be supplied through the main-rotor shaft; the revised value of main-rotor shaft power is then 93.9 horsepower.

If a particularly rigorous treatment is desired, the difference between the auxiliary-rotor values of  $(D/L)_0 + (D/L)_1$  and  $P/L$  should be converted into a drag-lift ratio based on the main-rotor lift, that is,  $0.049 \frac{102.7}{3140}$  or 0.002 for the present case. This value should then be added to the original value of  $(D/L)_p$  used in the main-rotor calculations, and the entire procedure repeated. Examination of the problem has shown, however, that the differences so obtained are negligible for normal ranges of variables, since the rotor profile drag-lift ratio is not particularly sensitive to the value of  $P/L$  used.

## CONCLUSIONS

1. The profile drag-lift ratio of a power-driven rotor in forward flight can be completely specified for various combinations of pitch angle, tip-speed ratio, and solidity by a series of charts for different values of power input. On the charts, the profile drag-lift ratio is plotted against the ratio of lift coefficient to solidity for specified values of pitch angle and tip-speed ratio.

2. For a rotor with rectangular untwisted blades, the theoretically derived charts indicate that one effect of increasing the shaft power input is to produce a moderate increase in the profile drag-lift ratio.

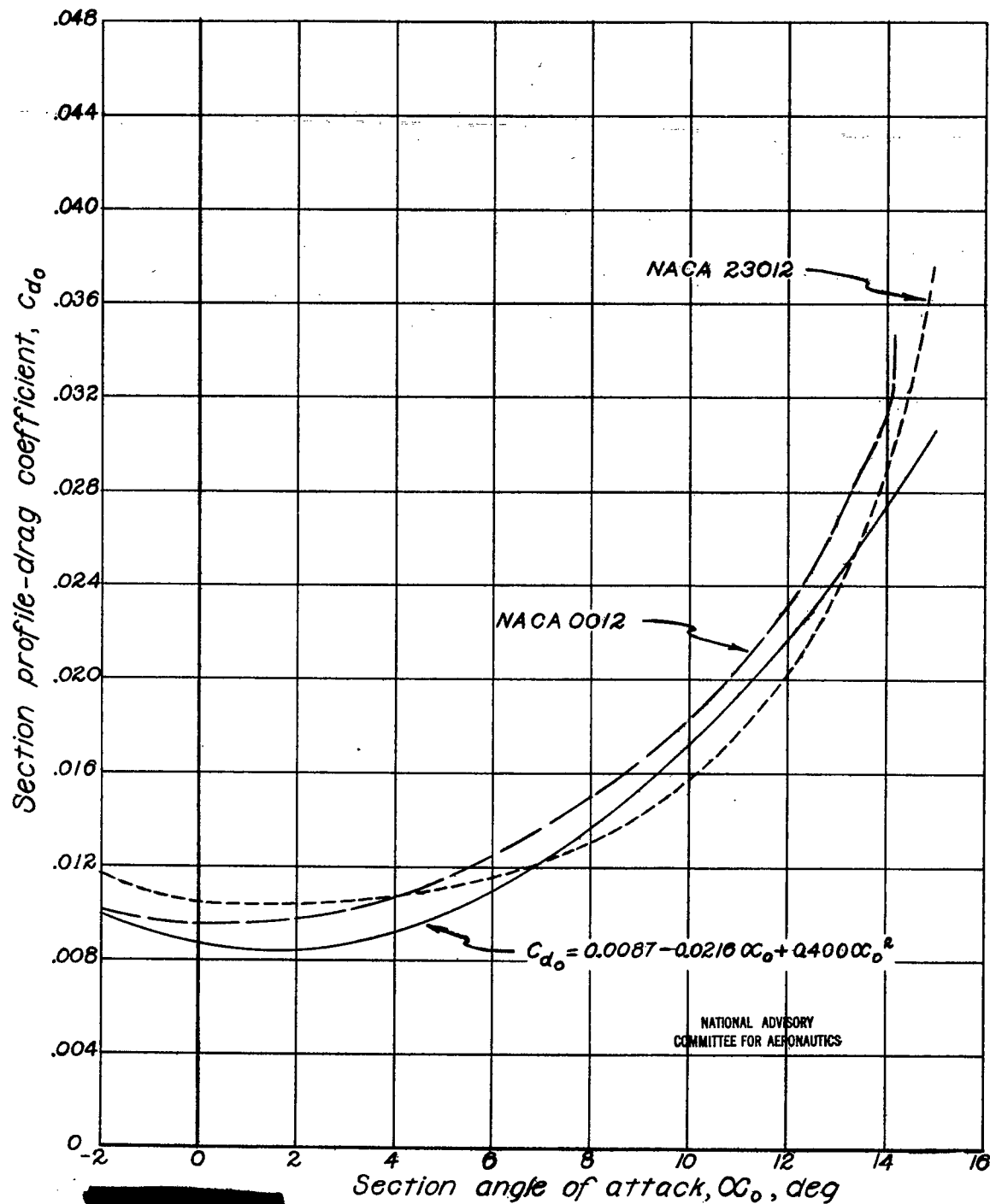
3. Regardless of the amount of power used, the optimum profile drag-lift ratio is obtained at the

highest pitch angles permitted by the high section angles of attack encountered on the retreating side of the rotor disk.

Langley Memorial Aeronautical Laboratory  
National Advisory Committee for Aeronautics  
Langley Field, Va.

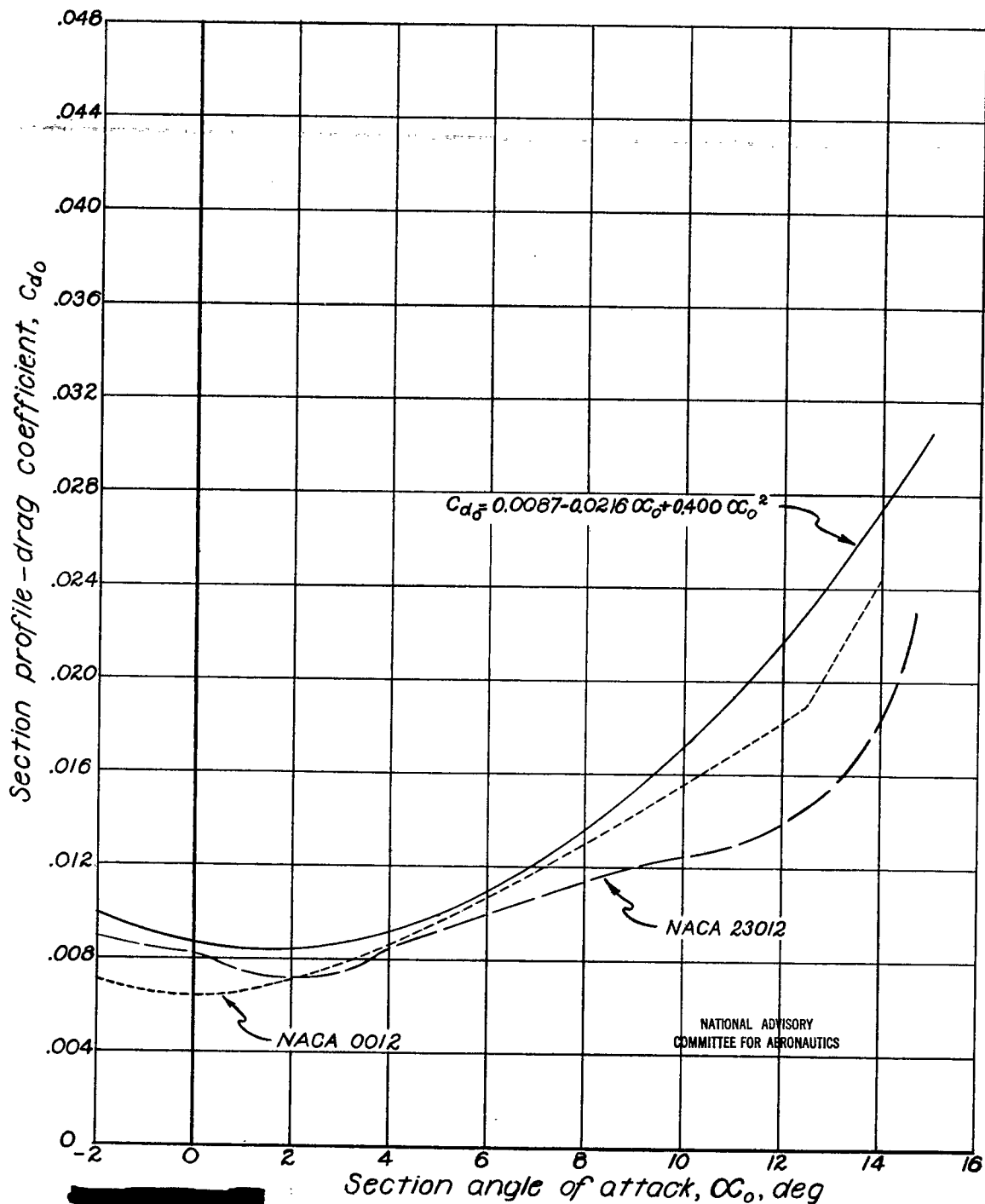
#### REFERENCES

1. Bailey, F. J., Jr.: A Simplified Theoretical Method of Determining the Characteristics of a Lifting Rotor in Forward Flight. NACA Rep. No. 716, 1941.
  2. Jacobs, Eastman N., and Sherman, Albert: Airfoil Section Characteristics as Affected by Variations of the Reynolds Number. NACA Rep. No. 586, 1937.
  3. Jacobs, Eastman N., and Clay, William C.: Characteristics of the N.A.C.A. 23012 Airfoil from Tests in the Full-Scale and Variable-Density Tunnels. NACA Rep. No. 530, 1935.
  4. Goett, Harry J., and Bullivant, W. Kenneth: Tests of N.A.C.A. 0009, 0012, and 0018 Airfoils in the Full-Scale Tunnel. NACA Rep. No. 647, 1938.
  5. Tetervin, Neal: Tests in the NACA Two-Dimensional Low-Turbulence Tunnel of Airfoil Sections Designed to Have Small Pitching Moments and High Lift-Drag Ratios. NACA CB No. 3113, 1943.
- [REDACTED]



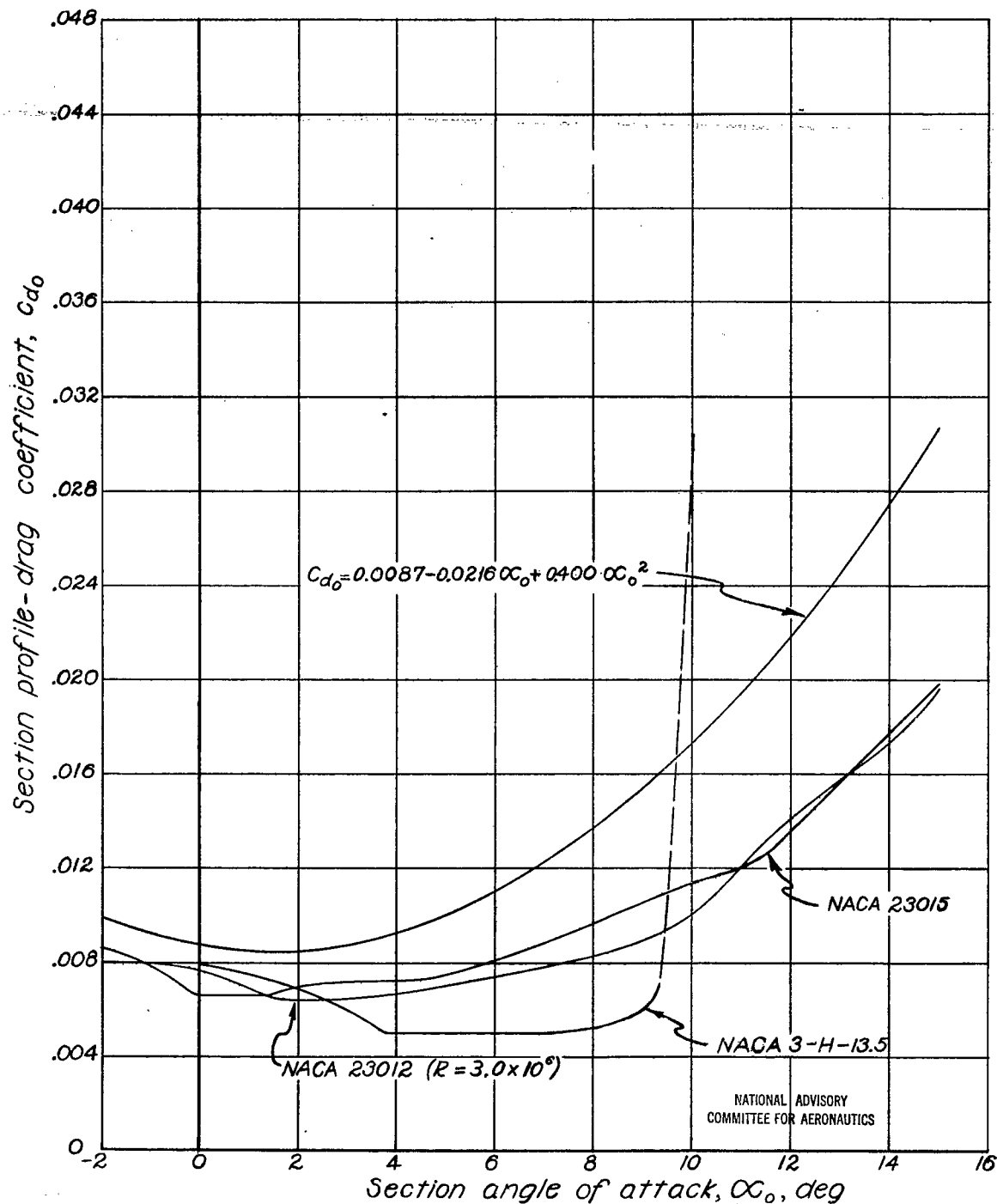
(a) Data from NACA variable-density tunnel; Reynolds number,  $2.6 \times 10^6$ ; reference 2.

Figure 1.- Comparison of the power-series profile-drag curve used in the analysis with experimental data on representative airfoil sections.



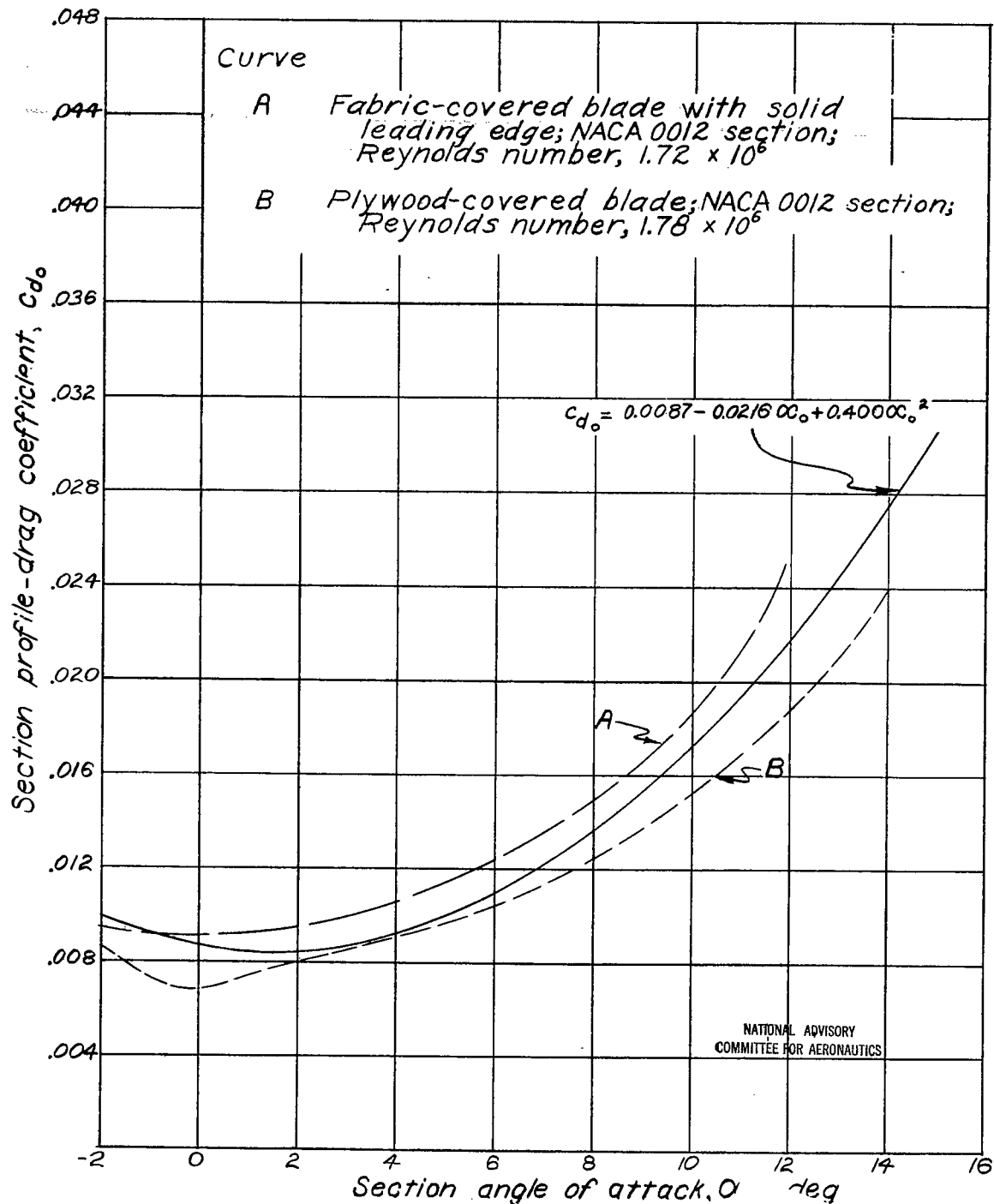
(b) Data from NACA full-scale tunnel; Reynolds number,  $3.4 \times 10^6$ ; references 3 and 4.

Figure 1.- Continued.



(c) Data from NACA two-dimensional low-turbulence tunnel and NACA two-dimensional low-turbulence pressure tunnel; Reynolds number,  $2.6 \times 10^6$ ; reference 5 and unpublished data.

Figure 1.- Continued.



(d) Data on practical-construction rotor-blade specimens, from NACA two-dimensional low-turbulence pressure tunnel; unpublished data.

Figure 1.- Concluded.

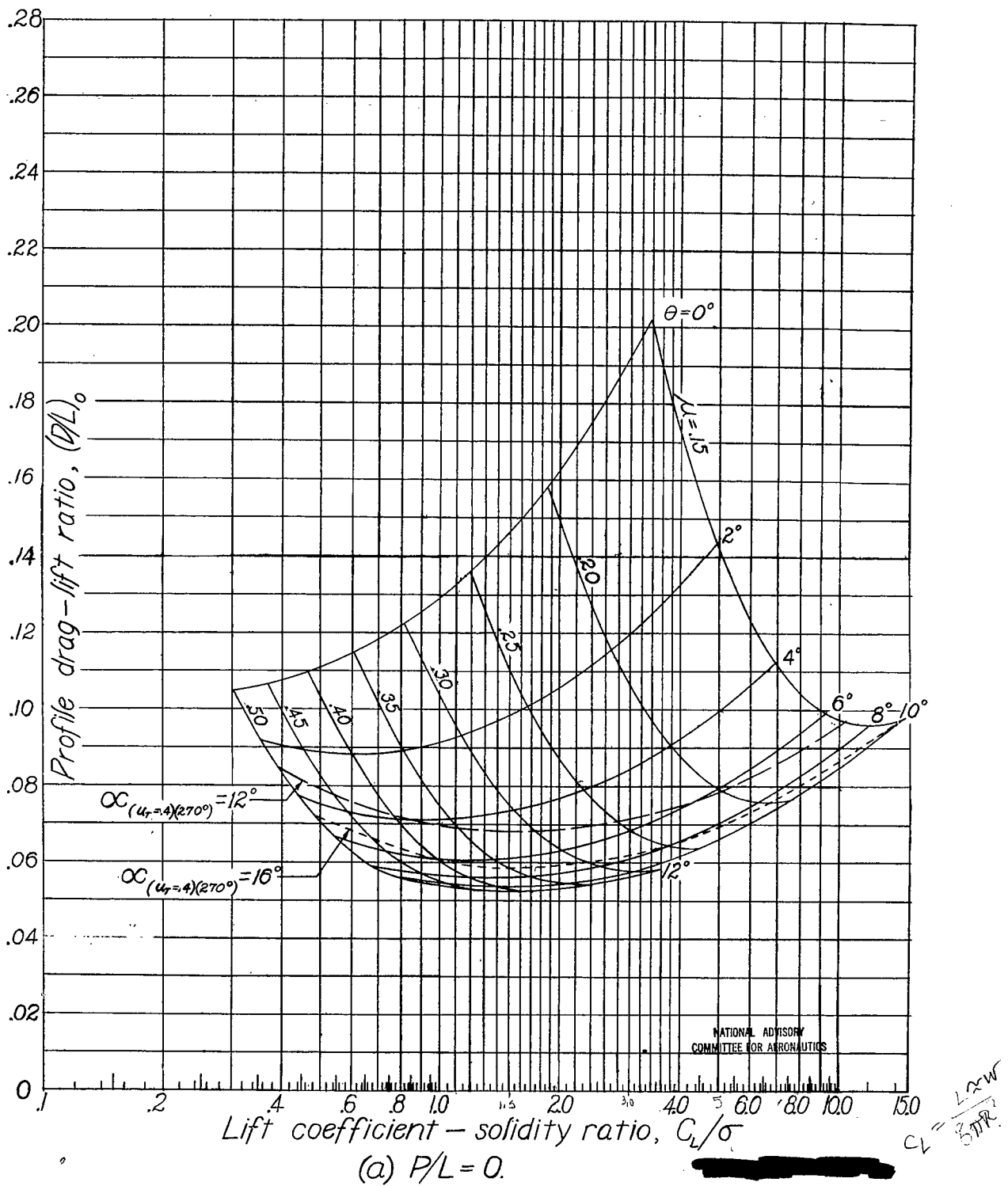


Figure 2.- Profile drag-lift ratio for sample rotor.

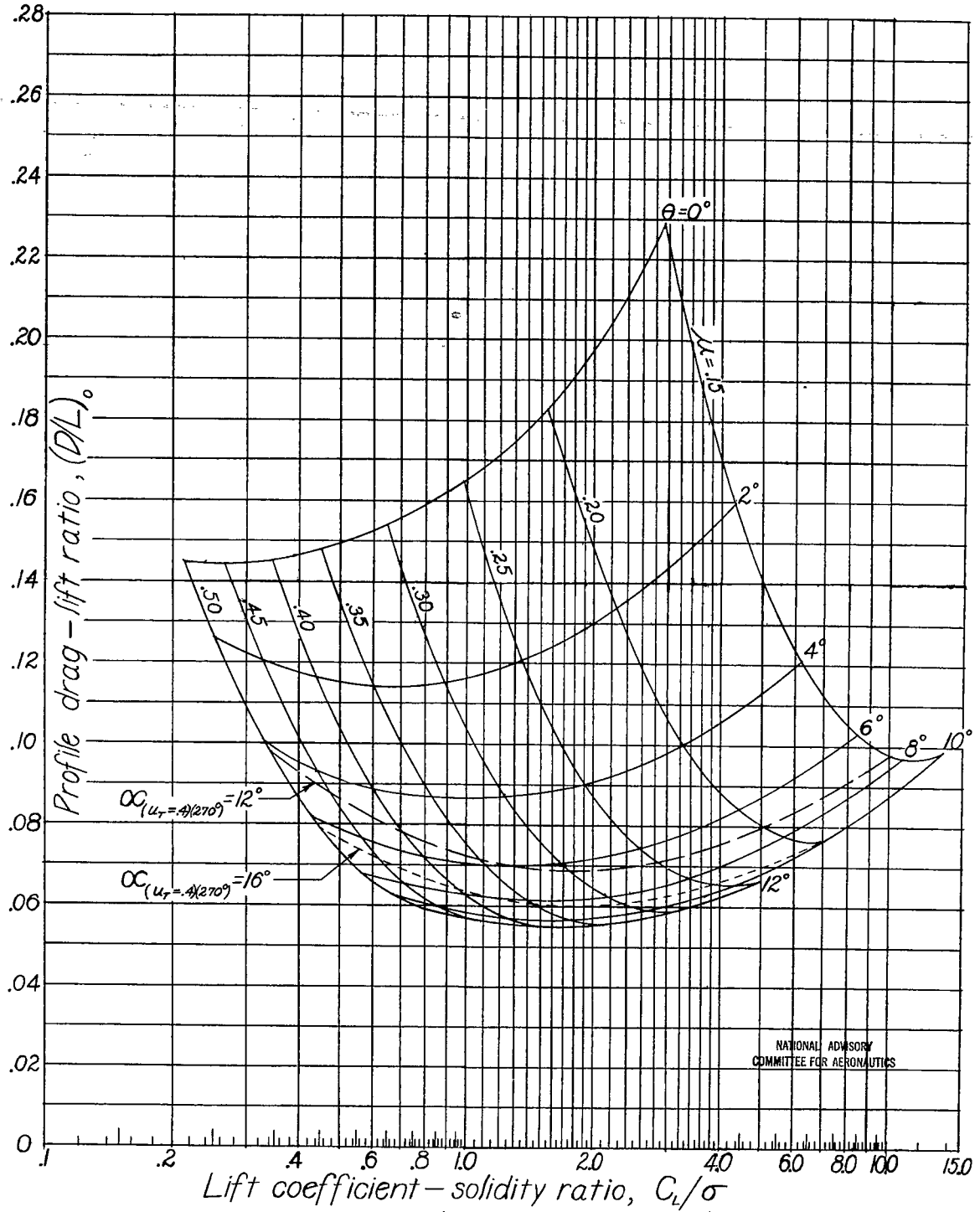
(b)  $P/L = .05$ .

Figure 2.- Continued.



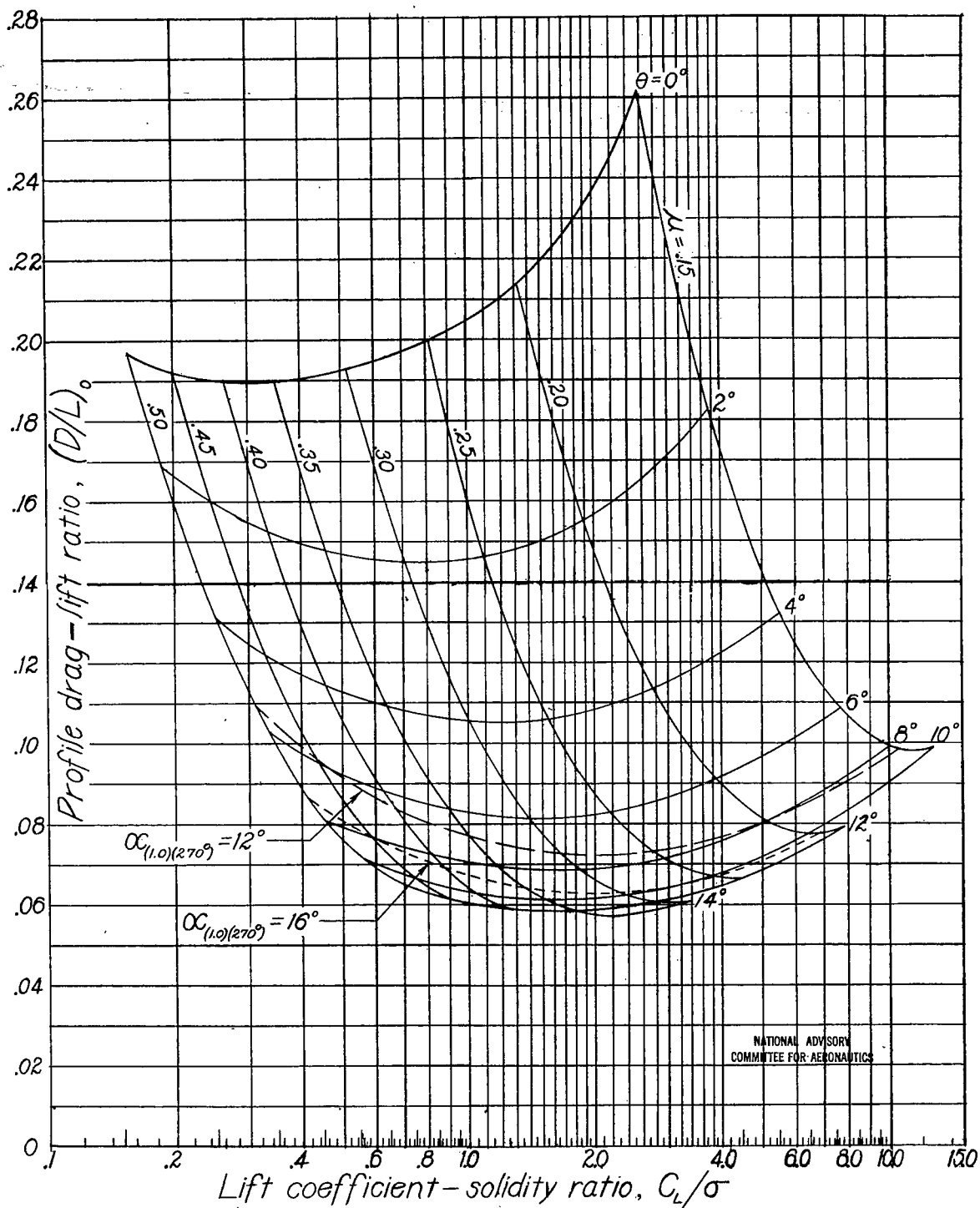
(c)  $P/L = .10$ .

Figure 2.- Continued.

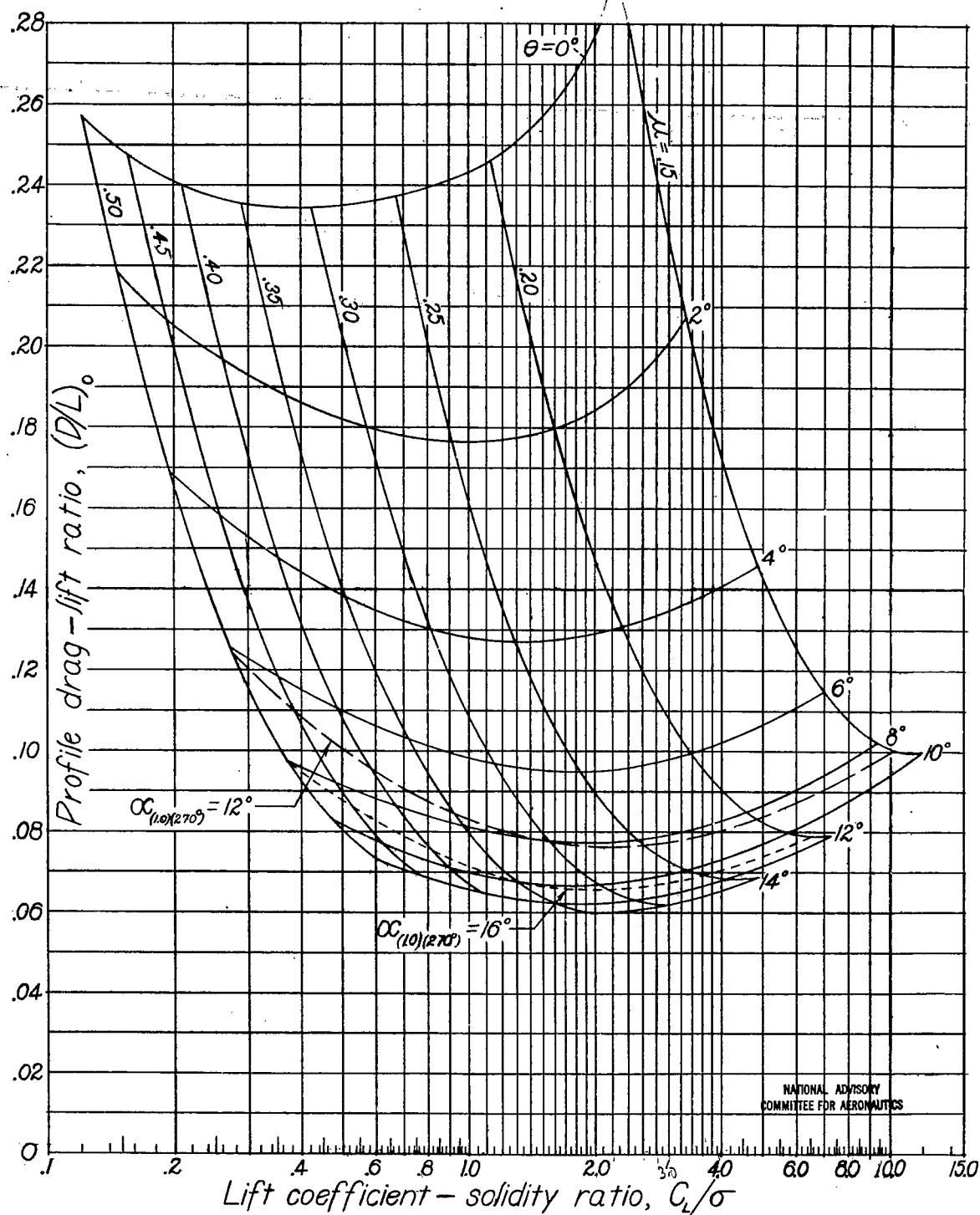
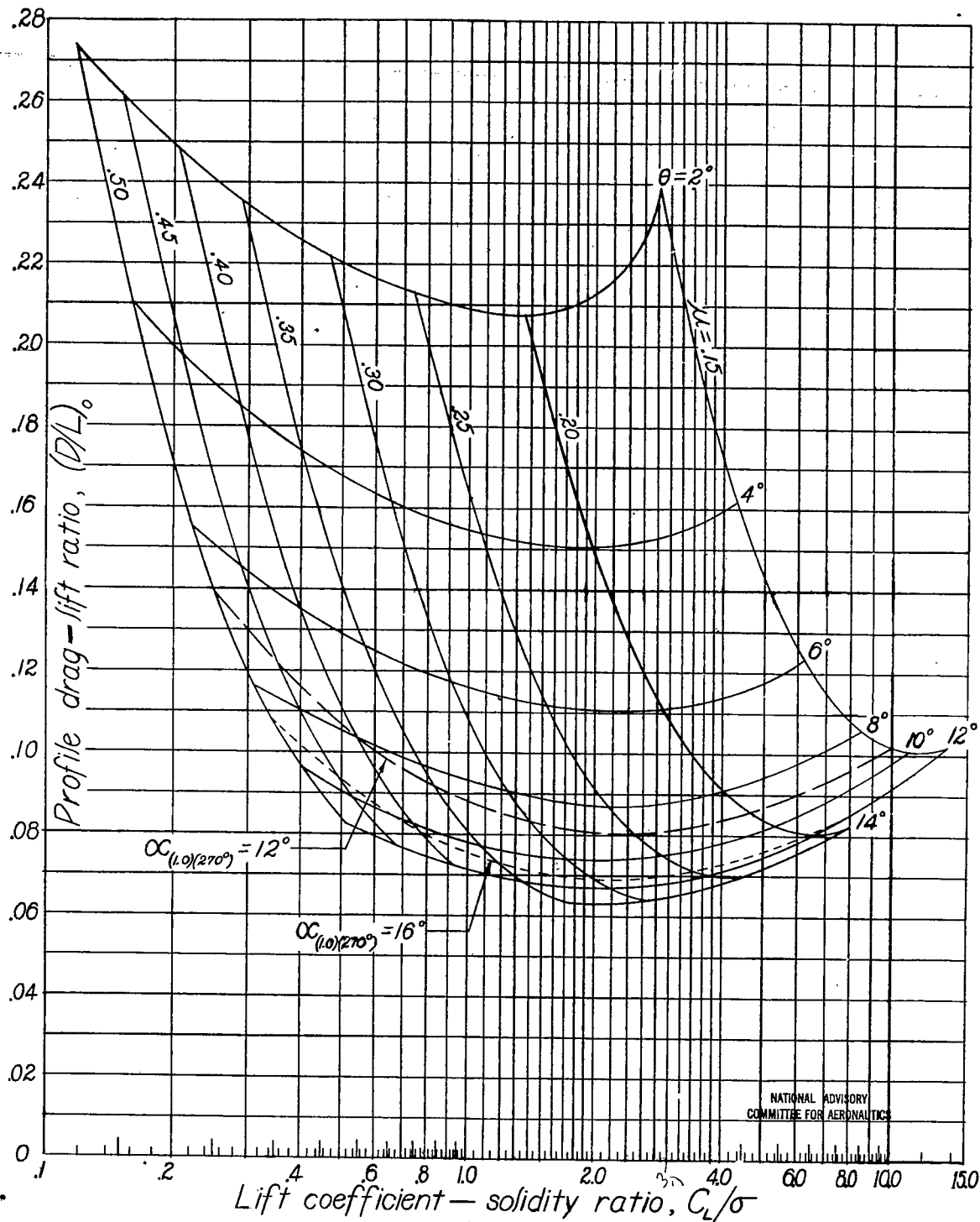


Figure 2.- Continued.



(e)  $P/L = 20$ .  
Figure 2.- Continued.

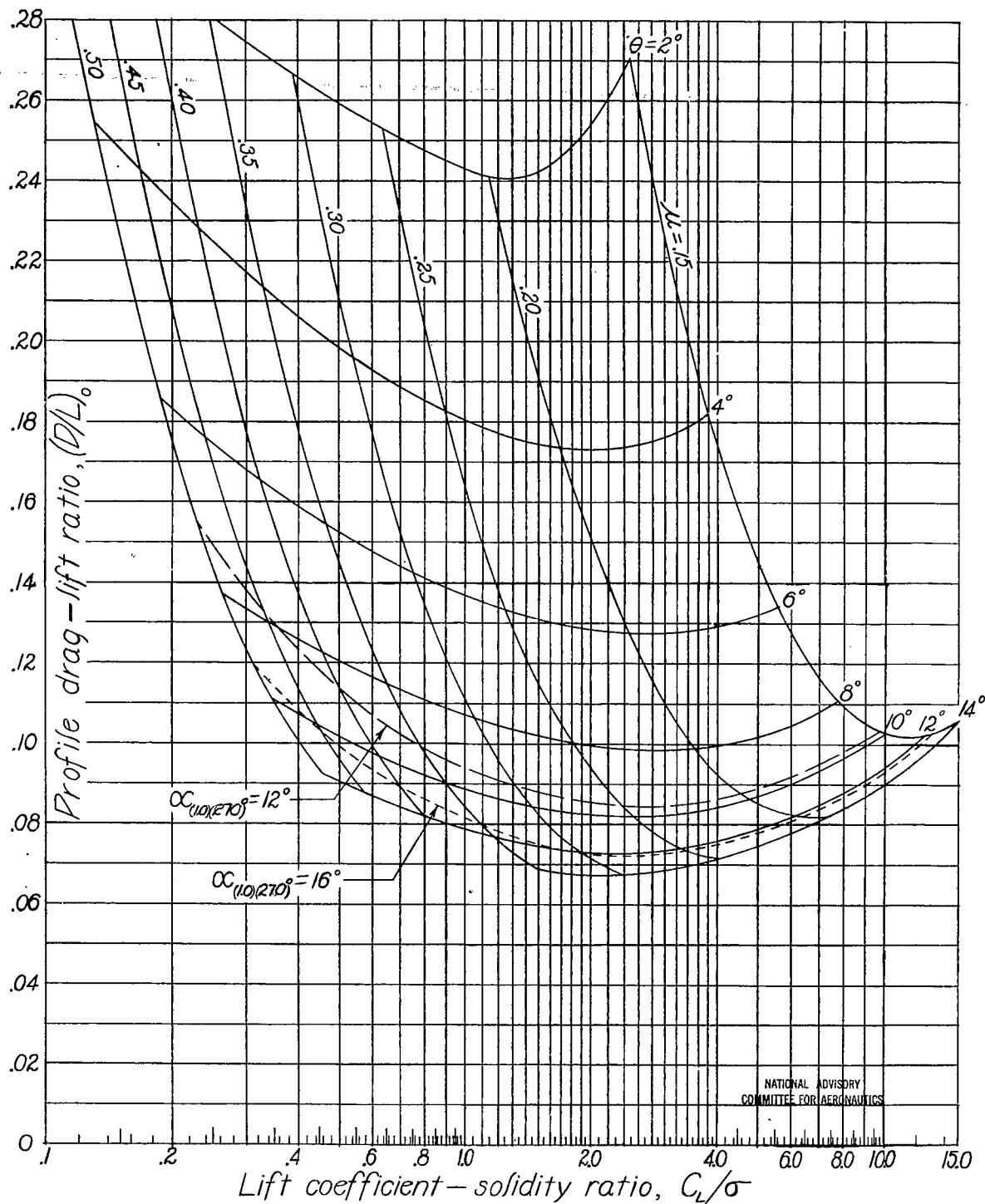
(f)  $P/L = .25$ .

Figure 2.- Continued.

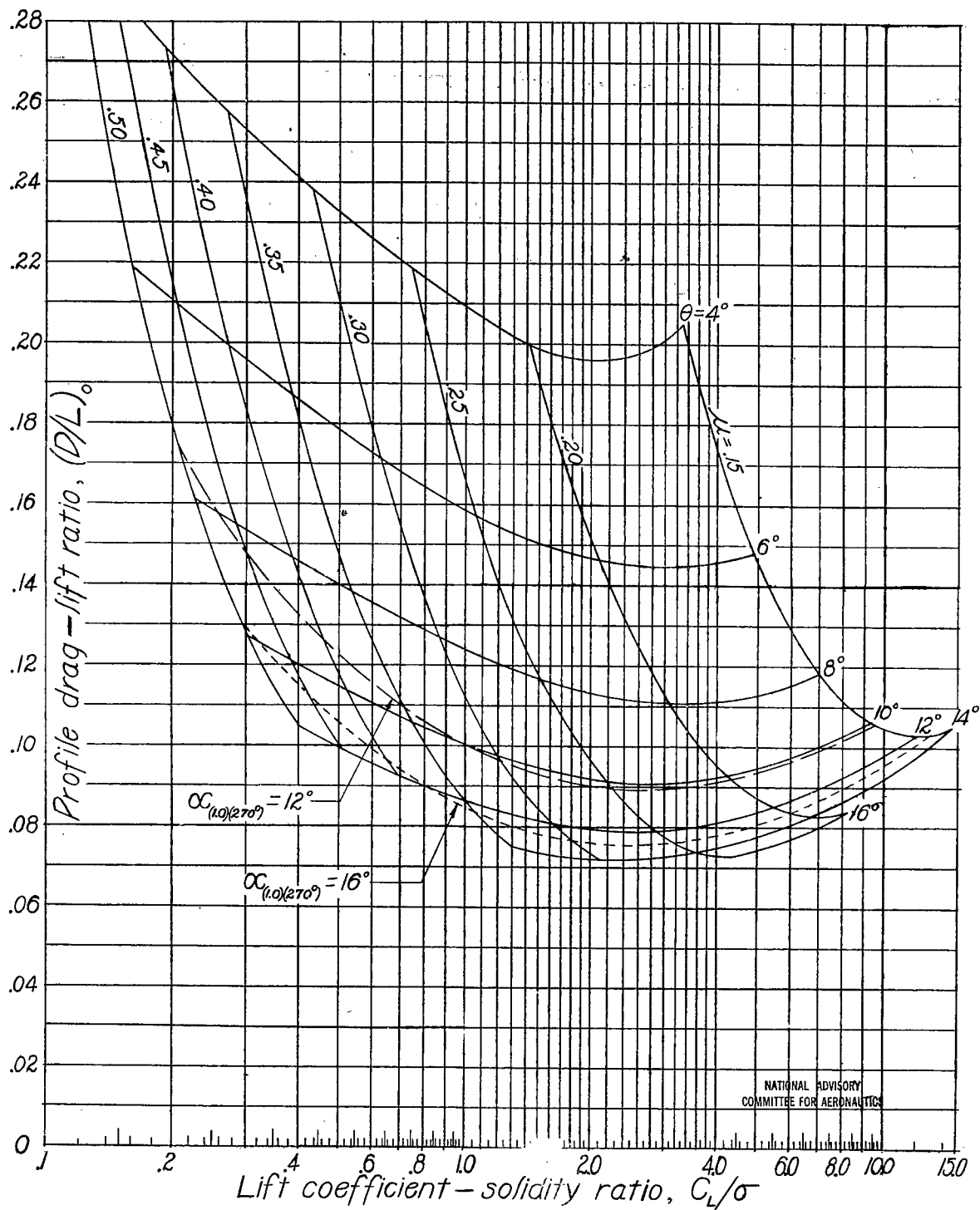
(g)  $P/L = .30$ 

Figure 2.- Continued.

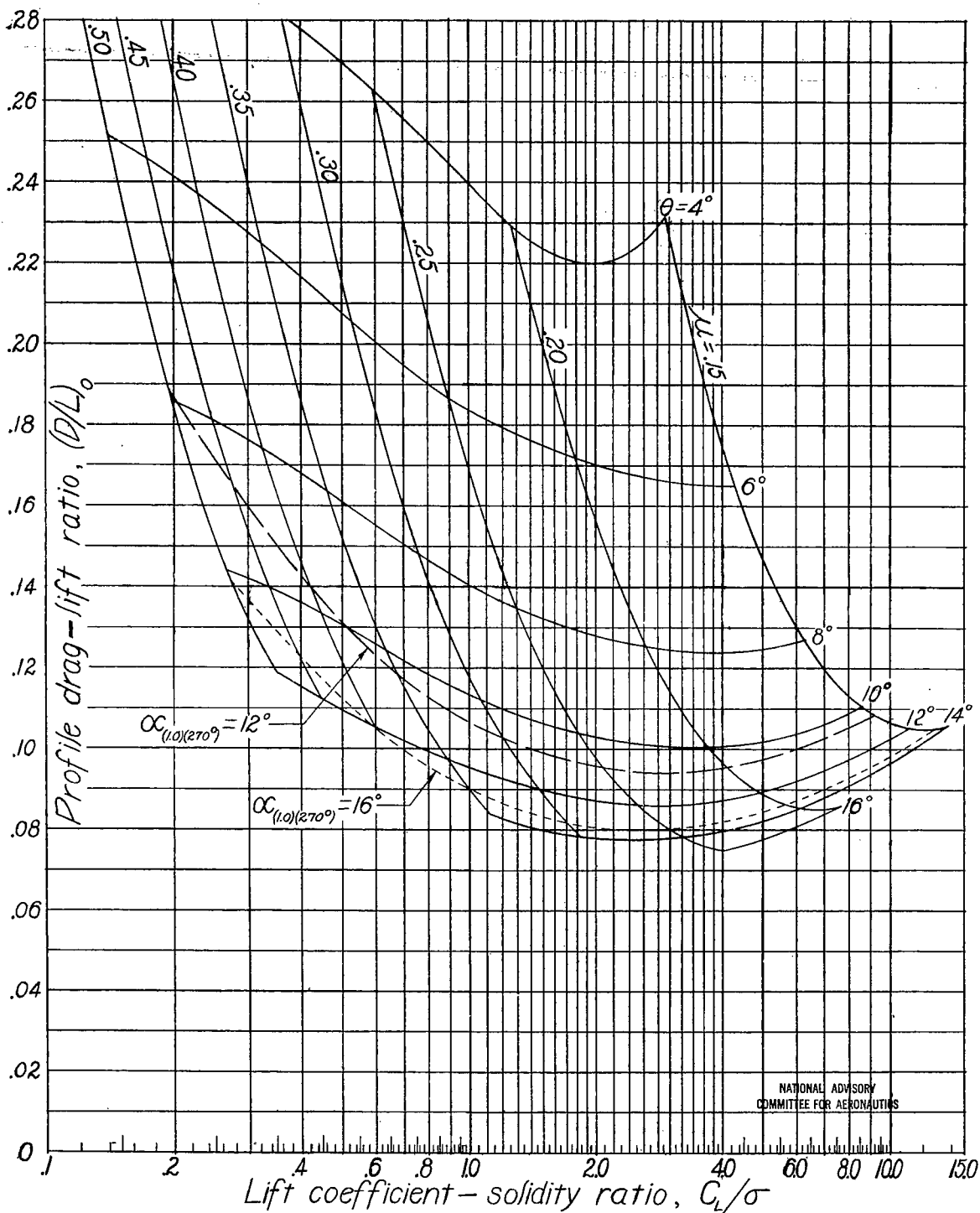
(h)  $P/L = .35$ .

Figure 2.- Continued.

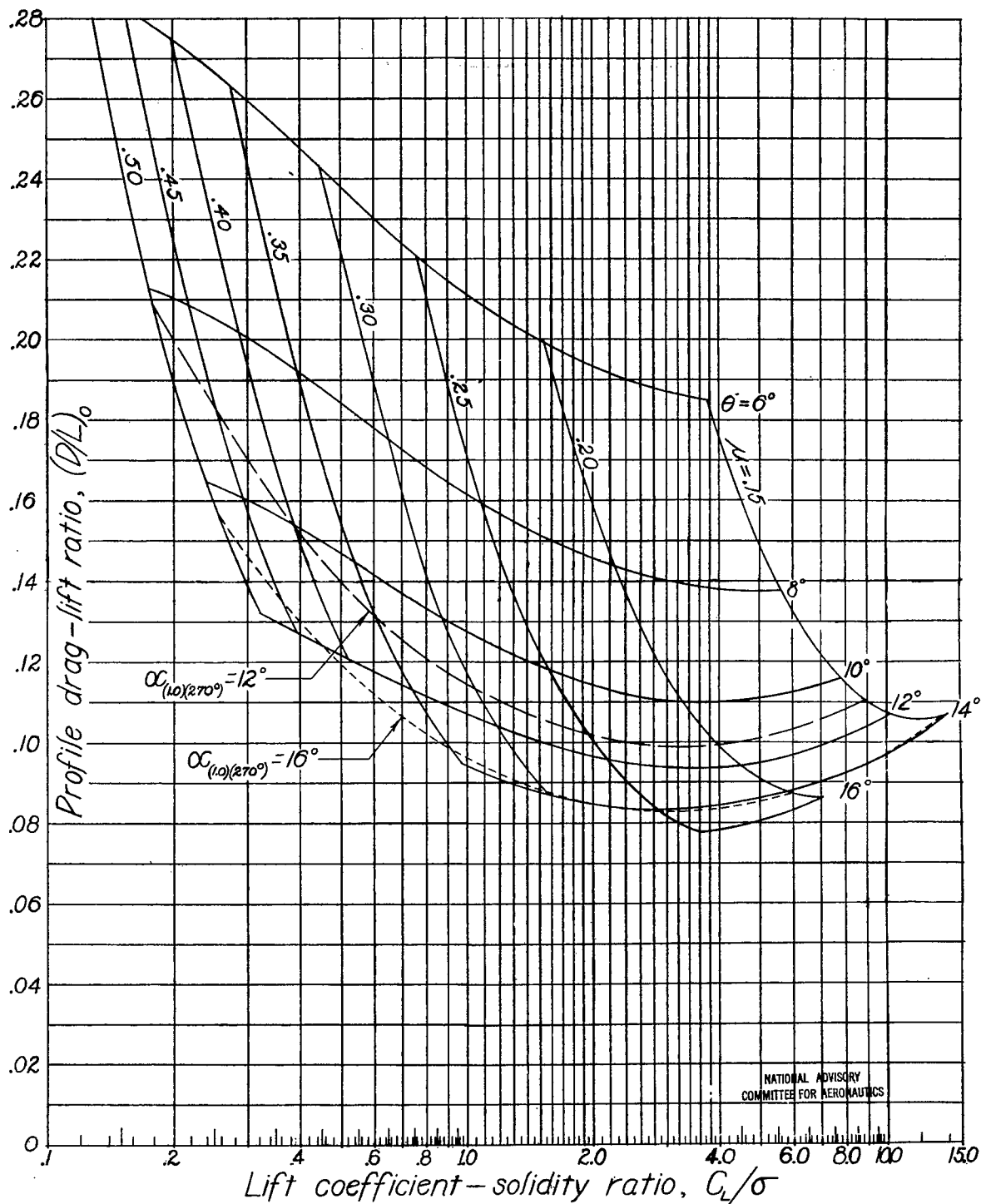
(i)  $P/L = 40$ .

Figure 2.- Continued.

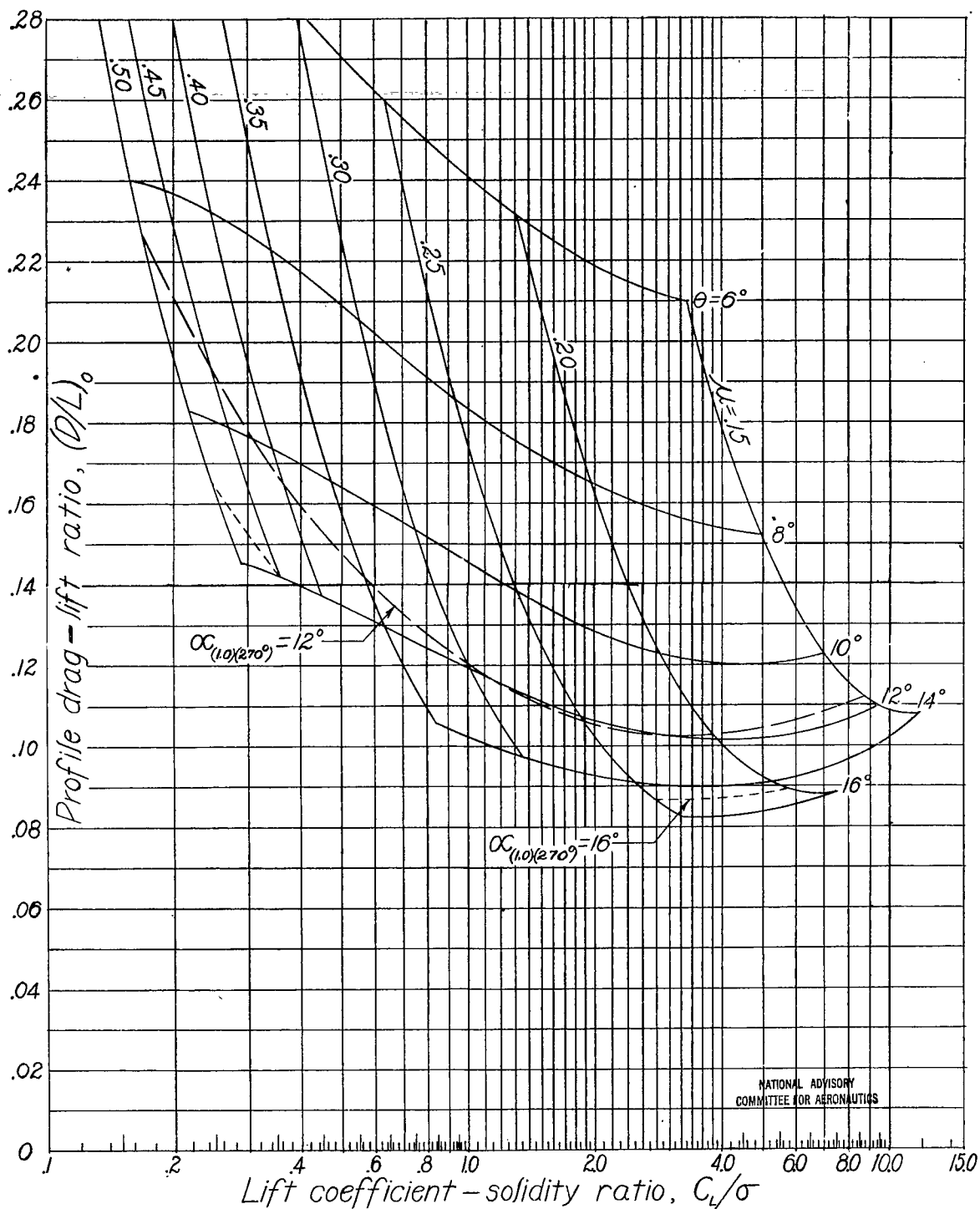
(j)  $P/L = .45$ .

Figure 2.- Continued.



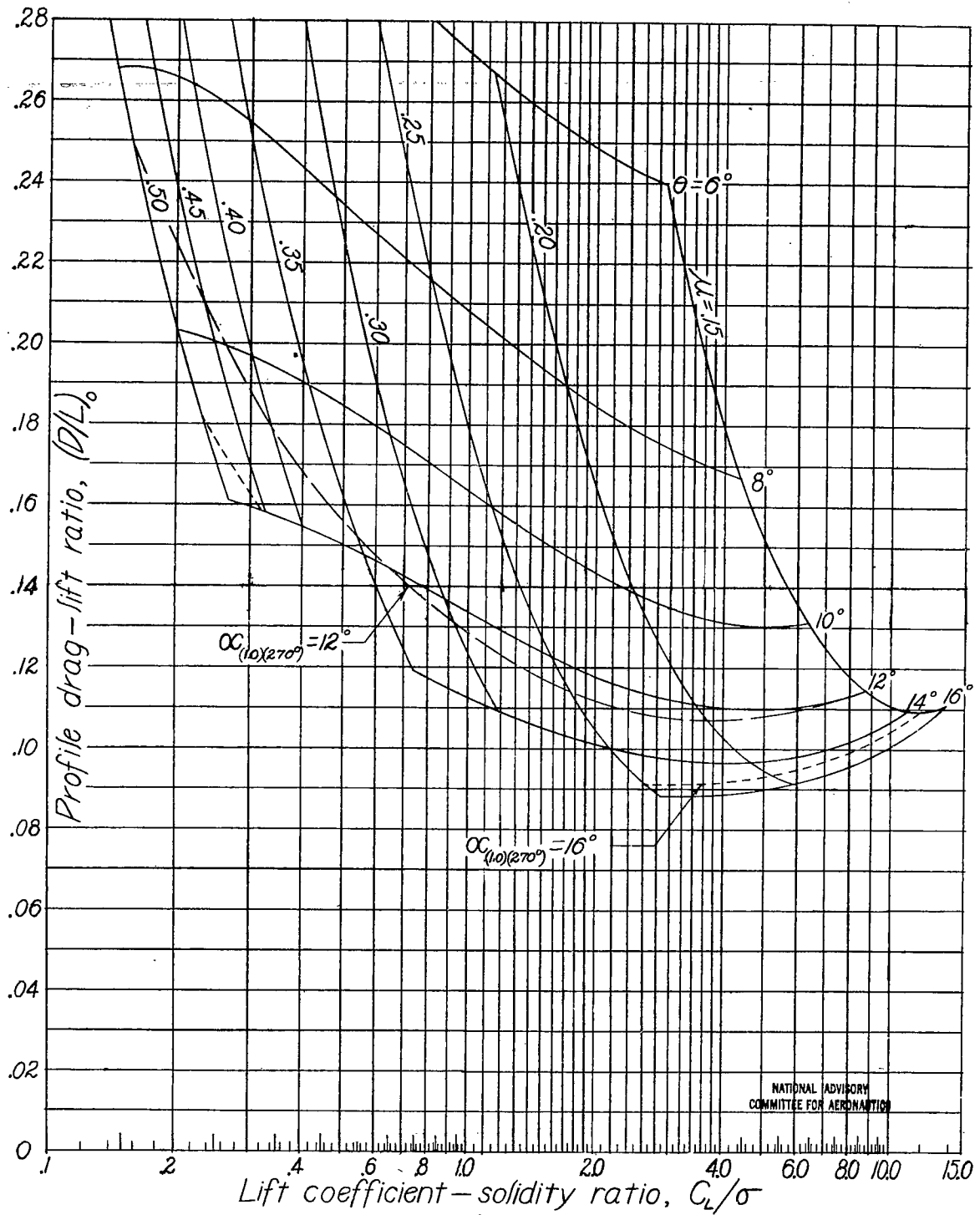
(k)  $P/L = .50$ .

Figure 2.- Concluded.